Journal of The Electrochemical Society, **156** (4) A260-A271 (2009)
0013-4651/2009/156(4)/A260/12/$23.00 © The Electrochemical Society

Mathematical Model Reformulation for Lithium-Ion Battery Simulations: Galvanostatic Boundary Conditions

Venkat R. Subramanian,[*,z] Vijayasekaran Boovaragavan,[,***] Venkatasailanathan Ramadesigan,[**] and Mounika Arabandi**

Department of Chemical Engineering, Tennessee Technological University, Cookeville, Tennessee 38505, USA

This paper presents an effective first step in the mathematical reformulation of physics-based lithium-ion battery models to improve computational efficiency. While the additional steps listed elsewhere [*Electrochem. Solid-State Lett.*, **10**, A225 (2007)] can be carried out to expedite the computation, the method described here is an effective first step toward efficient reformulation of lithium-ion battery models to expedite computation. The battery model used for the simulation is derived from the first principles as an isothermal pseudo-two-dimensional model with volume-averaged equations for the solid phase and with incorporation of concentrated solution theory, porous electrode theory, and with due consideration to the variations in electronic/ionic conductivities and diffusivities. The nature of the model and the structure of the governing equations are exploited to facilitate model reformulation, yielding efficient and accurate numerical computations.
 [DOI: 10.1149/1.3065083]

Manuscript submitted August 19, 2008; revised manuscript received December 10, 2008. Published January 30, 2009.

Mathematical modeling of lithium-ion batteries involves the specification of the dependent variables of interest (e.g., solution-phase concentration) and the first principles based derivation of governing equations for these dependent variables (based on the physics of the battery system) with specification of boundary/initial conditions and nonlinear expressions for transport/kinetic parameters. Doyle et al.[1] developed a model for a lithium-ion sandwich that consists of a porous electrode, separator, and a current collector. This model is based on the concentrated solution theory.[2] This important effort paved the way for a number of similar models, because it is general enough to incorporate further developments in a battery system.[3-13] Reviews of models for lithium-ion batteries can be found elsewhere in the literature.[10-12] Table I depicts a pseudo-two-dimensional isothermal model for a lithium-ion battery which has been converted to a one-dimensional (1D) model using approximations for solid-state diffusion.[14-16] Table II presents the various expressions used in the model. The parameters used for the simulation are given in Table III. For analysis and control of lithium-ion batteries in hybrid environments (with a fuel cell, capacitor, or electrical components), there is a need to simulate state of charge, state of health, and other parameters of lithium-ion batteries in milliseconds. Rigorous physics-based models take a few seconds up to a few minutes to simulate discharge curves, depending on the solvers, routines, computers, etc. Circuit-based or empirical models (based on the past data) can be simulated in milliseconds. However, these models fail at various operating conditions, and use of these models might cause abuse or under-utilization of electrochemical power sources. This paper presents the mathematical analysis for reformulation of physics-based models.

Lithium-Ion Battery Model Complexities

Simulation of lithium-ion battery models requires simultaneous evaluation of concentration and potential fields, in both solid as well as liquid phases. In addition, the porous nature of the battery electrodes leads to highly nonlinear and heterogeneous electrochemical reaction kinetics. The transport properties such as ionic and electronic conductivities and lithium-ion diffusivity might also vary during the course of electrochemical reactions. It has been well established that volume-averaging[17,18] coupled with polynomial approximation for the solid phase works well at low-to-medium rates of discharge.[19,20] Hence, the model considered is given in Table I, where the solid-phase diffusion equation is addressed with this approximation. The readers are advised at this point that the volume-averaged equations are not valid at short times and pulse charges/discharges. The solid-phase equations should be reformulated in an efficient form before reformulation is done for the other variables. However, this paper focuses on reformulation in the x direction, and hence the discussion is limited to volume-averaged equations for the solid-phase equation.

In general, the numerical simulation of lithium-ion battery models is done by discretizing all the variables in the x coordinate using finite difference. Let us assume that we discretize the cathode, separator, and anode into 50 equally spaced node points in linear length scale, i.e., in x. The cathode now has 50 differential equations for the electrolyte concentration, 50 algebraic equations for the electrolyte potential (potential in the electrolyte phase), and 50 algebraic equations for the solid-phase potential. Also, we have 50 differential and 50 algebraic equations for the solid-phase average and surface concentrations. Thus, for a single porous electrode (say, for cathode), we have 250 differential algebraic equations (DAEs). Following the same number of node points in x, the separator now has 50 differential equations for the electrolyte concentration and 50 algebraic equations for the electrolyte potential. The anode is discretized similar to the cathode and has a total of $5 \times 50 = 250$ DAEs to solve. Thus, the number of DAEs to be solved for the full-order model is $5 \times 50 + 2 \times 50 + 5 \times 50 = 600$ DAEs.

Given the number of space-discretized equations involved as 600 DAEs, milliseconds simulation of the lithium-ion battery model is impractical if standard discretization schemes are directly employed. Real-time optimization and feedback control of the sensitive lithium-ion battery, where the health of the battery is vital to the very operation of the device, requires quick-solving models that can give an accurate account of the battery variables. The full physics-based model described in Table I is therefore not the best candidate for these requirements. In this investigation, consideration has been given for various possible techniques to solve for dependent variables without losing accuracy.

The authors have given general information on their reformulation of lithium-ion battery models to enable milliseconds simulation.[21] However, this article gives specific information on a particular method of reformulation for dependent variables in the x direction, and it can be further improved in terms of computational efficiency. In the next section, details on the approach used to reformulate each dependent variable in each region of the lithium-ion battery model are provided.

The authors would like to mention that there is a significant difference between approximation for a model and reformulation for

* Electrochemical Society Active Member.
** Electrochemical Society Student Member.
*** ECS Oronzio de Nora Industrial Electrochemistry Fellowship Award Recipient.
z E-mail: vsubramanian@tntech.edu

Table I. Governing equations for a lithium-ion battery.

Region	Eq. no.	Governing equations	Boundary conditions
Positive electrode	1	$\varepsilon_p \frac{\partial c}{\partial t} = D_{\text{eff,p}} \frac{\partial^2 c}{\partial x^2} + a_p(1-t_+)j_p$ initial condition $c\|_{t=0} = c_0$	$-D_{\text{eff,p}} \frac{\partial c}{\partial x}\|_{x=0} = 0$ and $-D_{\text{eff,p}} \frac{\partial c}{\partial x}\|_{x=l_{p,-}} = -D_{\text{eff,s}} \frac{\partial c}{\partial x}\|_{x=l_{p,+}}$
	2	$-\sigma_{\text{eff,p}} \frac{\partial \Phi_1}{\partial x} - \kappa_{\text{eff,p}} \frac{\partial \Phi_2}{\partial x} + \frac{2\kappa_{\text{eff,p}}RT}{F}(1-t_+)\frac{\partial \ln c}{\partial x} = I$	$-\kappa_{\text{eff,p}} \frac{\partial \Phi_2}{\partial x}\|_{x=0} = 0$ and $-\kappa_{\text{eff,p}} \frac{\partial \Phi_2}{\partial x}\|_{x=l_{p,-}} = -\kappa_{\text{eff,s}} \frac{\partial \Phi_2}{\partial x}\|_{x=l_{p,+}}$
	3	$\sigma_{\text{eff,p}} \frac{\partial^2 \Phi_1}{\partial x^2} = a_p F j_p$	$\frac{\partial \Phi_1}{\partial x}\|_{x=0} = -\frac{I}{\sigma_{\text{eff,p}}}$ and $\Phi_1 = 4.2$
	4	$\frac{d}{dt}c_s^{\text{ave}} + 3\frac{j_p}{R_p} = 0$ and $\frac{D_{s,p}}{R_p}(c_s^{\text{surf}} - c_s^{\text{ave}}) = -\frac{j_p}{5}$ initial condition $c_s^{\text{ave}}\|_{t=0} = c_{s,\max,p}$	
Separator	5	$\varepsilon_s \frac{\partial c}{\partial t} = D_{\text{eff,s}} \frac{\partial^2 c}{\partial x^2}$	$-D_{\text{eff,p}} \frac{\partial c}{\partial x}\|_{x=l_{p,-}} = -D_{\text{eff,s}} \frac{\partial c}{\partial x}\|_{x=l_{p,+}}$ and $D_{\text{eff,s}} \frac{\partial c}{\partial x}\|_{x=l_p+l_{s,-}} = -D_{\text{eff,n}} \frac{\partial c}{\partial x}\|_{x=l_p+l_{s,+}}$
	6	$I = -\kappa_{\text{eff,s}} \frac{\partial \Phi_2}{\partial x} + \frac{2\kappa_{\text{eff,s}}RT}{F}(1-t_+)\frac{\partial \ln c}{\partial x}$	$-\kappa_{\text{eff,p}} \frac{\partial \Phi_2}{\partial x}\|_{x=l_{p,-}} = -\kappa_{\text{eff,s}} \frac{\partial \Phi_2}{\partial x}\|_{x=l_{p,+}}$ and $-\kappa_{\text{eff,s}} \frac{\partial \Phi_2}{\partial x}\|_{x=l_p+l_{s,-}} = -\kappa_{\text{eff,n}} \frac{\partial \Phi_2}{\partial x}\|_{x=l_p+l_{s,+}}$
Negative electrode	7	$\varepsilon_n \frac{\partial c}{\partial t} = D_{\text{eff,n}} \frac{\partial^2 c}{\partial x^2} + a_n(1-t_+)j_n$ initial condition $c\|_{t=0} = c_0$	$-D_{\text{eff,s}} \frac{\partial c}{\partial x}\|_{x=l_p+l_{s,-}} = -D_{\text{eff,n}} \frac{\partial c}{\partial x}\|_{x=l_p+l_{s,+}}$ and $-D_{\text{eff,n}} \frac{\partial c}{\partial x}\|_{x=l_p+l_s+l_n} = 0$
	8	$-\sigma_{\text{eff,n}} \frac{\partial \Phi_1}{\partial x} - \kappa_{\text{eff,n}} \frac{\partial \Phi_2}{\partial x} + \frac{2\kappa_{\text{eff,n}}RT}{F}(1-t_+)\frac{\partial \ln c}{\partial x} = I$	$-\kappa_{\text{eff,s}} \frac{\partial \Phi_2}{\partial x}\|_{x=l_p+l_{s,-}} = -\kappa_{\text{eff,n}} \frac{\partial \Phi_2}{\partial x}\|_{x=l_p+l_{s,+}}$ and $\frac{\partial \Phi_2}{\partial x}\|_{x=l_p+l_s+l_n} = 0$
	9	$\sigma_{\text{eff,n}} \frac{\partial^2 \Phi_1}{\partial x^2} = a_n F j_n$	$-\sigma_{\text{eff,n}} \frac{\partial \Phi_1}{\partial x}\|_{x=l_p+l_s} = 0$ and $\frac{\partial \Phi_1}{\partial x}\|_{x=l_p+l_s+l_n} = -\frac{I}{\sigma_{\text{eff,n}}}$
	10	$\frac{d}{dt}c_s^{\text{ave}} + 3\frac{j_n}{R_n} = 0$ and $\frac{D_{s,n}}{R_p}(c_s^{\text{surf}} - c_s^{\text{ave}}) = -\frac{j_n}{5}$ initial condition $c_s^{\text{ave}}\|_{t=0} = c_{s,\max,n}$	

Table II. Expressions used in the lithium-ion battery model given by Table I.

$$\kappa_{\text{eff},i} = \varepsilon_i^{\text{brugg}_i}\left(4.1253 \times 10^{-2} + 5.007 \times 10^{-4}c - 4.7212 \times 10^{-7}c^2 + 1.5094 \times 10^{-10}c^3 - 1.6018 \times 10^{-14}c^4\right)$$
$i = \text{p,s,n,}$

$$\sigma_{\text{eff},i} = \sigma_i(1 - \varepsilon_i - \varepsilon_{\text{f},i}),\ i = \text{p,n}$$

$$D_{\text{eff},i} = D\varepsilon_i^{\text{brugg}_i},\ i = \text{p,s,n}$$

$$a_i = \frac{3}{R_i}(1 - \varepsilon_i - \varepsilon_{\text{f},i}),\ i = \text{p,n}$$

$$j_p = 2k_p(c_{s,\max,p} - c_{s,p}|_{r=R_p})^{0.5}\, c_{s,p}|_{r=R_p}^{0.5} c^{0.5} \sinh\left[\frac{0.5F}{RT}(\Phi_1 - \Phi_2 - U_p)\right]$$

$$U_p = \frac{-4.656 + 88.669\theta_p^2 - 401.119\theta_p^4 + 342.909\theta_p^6 - 462.471\theta_p^8 + 433.434\theta_p^{10}}{-1.0 + 18.933\theta_p^2 - 79.532\theta_p^4 + 37.311\theta_p^6 - 73.083\theta_p^8 + 95.96\theta_p^{10}}$$
where $\theta_p = c_{s,p}|_{r=R_p}/c_{s,p,\max}$

$$j_n = 2k_n(c_{s,\max,n} - c_{s,n}|_{r=R_n})^{0.5}\, c_{s,n}|_{r=R_n}^{0.5} c^{0.5} \sinh\left[\frac{0.5F}{RT}(\Phi_1 - \Phi_2 - U_n + FR_{\text{SEI}}j_n)\right]$$

$$U_n = 0.7222 + 0.1387\theta_n + 0.029\theta_n^{0.5} - \frac{0.0172}{\theta_n} + \frac{0.0019}{\theta_n^{1.5}} + 0.2808\exp(0.90 - 15\theta_n) - 0.7984\exp(0.4465\theta_n - 0.4108)$$
where $\theta_n = c_{s,n}|_{r=R_n}/c_{s,n,\max}$

the same. For example, a series solution for a differential equation with a fixed number of terms in the series is an approximation for a model. However, if enough terms are chosen and if the series solution is developed to make sure that the solution has converged for any set of parameters or operating conditions, it is an effective model-reformulation approach because the accuracy is not lost.

Model reformulation is an active area of research for many engineering and science fields.[22] There are standard methods available in the literature for reducing the given set of coupled partial-differential equations (PDEs) to reduced order models with different levels of accuracy and details. Proper orthogonal discretization (POD) uses the full numerical solution to fit a reduced set of eigenvalues and nodes to get a meaningful solution with a reduced number of equations.[23] However, this method requires rigorous numerical solutions to build the POD reduced-order models. Also, when the operating current is doubled, the boundary conditions are changed, or if the parameter values are changed significantly, the POD model needs to be reconstructed.

The approach presented in this paper is analytical and is the result of doing analytical mathematical analysis, and hence it can be used confidently for parameter estimation and control purposes. This method can be considered as mathematical model reformulation. The method described for the variables in the x coordinates in this paper is equivalent to an analytical solution, applicable for even higher rates of discharge and other operating conditions (pulses, constant potential, and constant power) provided an efficient approximation is used.

Mathematical Analysis for Efficient Model Reformulation

This section describes the step-by-step mathematical details that reduce the 12 coupled nonlinear multiple PDEs from rigorous bat-

Table III. Parameters used for the simulation ($LiCoO_2$ and LiC_6 system).

Symbol	Unit	Positive electrode	Separator	Negative electrode
σ_i	S/m	100		100
$\varepsilon_{f,i}$		0.025		0.0326
ε_i		0.385	0.724	0.485
Brugg			4	
$D_{s,i}$	m^2/s	1.0×10^{-14}		3.9×10^{-14}
D	m^2/s		7.5×10^{-10}	
k_i	$Mol/(s\ m^2)/(mol/m^3)^{1+\alpha a,i}$	2.334×10^{-11}		5.0307×10^{-11}
$c_{s,i,max}$	mol/m^3	51554		30555
$c_{s,i0}$	mol/m^3	0.4955×51554		0.8551×30555
c_0	mol/m^3		1000	
R_p	m	2.0×10^{-6}		2.0×10^{-6}
l_i	m	80×10^{-6}	25×10^{-6}	88×10^{-6}
R_{SEI}	$\Omega\ m^2$			0.0
t_+			0.363	
F	C/mol		96487	
R	J/(mol K)		8.314	
T	K		298.15	

tery modeling to a very few DAEs to achieve milliseconds simulation for online control and optimization. The approach involves considering each dependent variable separately and finding a suitable mathematical method to minimize the computational burden associated with that particular variable. While doing such an investigation, it is necessary to keep the dependency of a chosen variable with other dependent/independent variables intact.

For the model considered in Table I, the following dependent variables are solved in x in each electrode: Φ_1, Φ_2, c, c_s^{ave}, and j_p. The governing equations for these five variables (varying with x) are

$$\sigma_{eff,p}\frac{\partial^2\Phi_1}{\partial x^2} = a_p F j_p \quad [11]$$

$$-\sigma_{eff,p}\frac{\partial\Phi_1}{\partial x} - \kappa_{eff,p}\frac{\partial\Phi_2}{\partial x} + \frac{2\kappa_{eff,p}RT}{F}(1-t_+)\frac{\partial \ln c}{\partial x} = I \quad [12]$$

$$\varepsilon_p\frac{\partial c}{\partial t} = D_{eff,p}\frac{\partial^2 c}{\partial x^2} + a_p(1-t_+)j_p \quad [13]$$

$$\frac{d}{dt}c_s^{ave} + 3\frac{j_p}{R_p} = 0 \quad [14]$$

where

$$j_p = 2k_p\left[c_{s,max,p} - \left(c_s^{ave} - \frac{j_p R_p}{5D_{s,p}}\right)\right]^{0.5}\left(c_s^{ave} - \frac{j_p R_p}{5D_{s,p}}\right)^{0.5} \times c^{0.5}\sinh\left[\frac{0.5F}{RT}(\Phi_1 - \Phi_2 - U_p)\right] \quad [15]$$

All of the above equations vary as a function of x and t. (c_s^{surf} can be obtained as a function of x and t from its equation given in Table I as a postcalculation after j_p is obtained). In the next section, the advantage of solving for j_p as opposed to c_s^{surf} is illustrated.

Instead of solving this model with 250 DAEs, for one porous electrode, this section illustrates one way to reduce the number of DAEs by performing various mathematical analyses. In our group, we have attempted and arrived at various possible ways of simulating this model, including finite-element method, finite difference in x solved using BANDJ and DASSL, orthogonal collocation, etc. By attempting various methods, we have finally arrived at efficient, and perhaps the two best possible, approaches for this system of equations characterized by its DAE nature. These reformulations are based on finite differences and polynomial representation and are discussed in detail below.

Finite difference formulation: Method for model reformulation.— In the literature, finite difference is the most commonly used method to discretize the spatial derivatives in the governing equations. In this section we provide the details for model reformulation if finite difference is used. The steps are described in detail for each variable. A flowchart describing the same is given in Fig. 1.

Solid-phase potential.— The governing equation for solid-phase potential is derived from Ohm's law and is given by Eq. 3 and 9 in Table I for positive and negative electrodes, respectively. If j_p is a constant, clearly Eq. 11 can be solved to obtain a closed-form solution. However, j_p is a nonlinear function of the dependent variables, as shown in Eq. 15. If finite difference is applied in the x direction, Eq. 11 can be written as

$$\sigma_{eff,p}\frac{\Phi 1_{i+1} - 2\Phi 1_i + \Phi 1_{i-1}}{h_1^2} = a_p F j_{pi} \quad i = 1 \ldots N \quad [16]$$

where N is the number of interior node points used. Equation 6 can be written in matrix form as

$$\boldsymbol{A\Phi}_1 = \boldsymbol{j}_p + \boldsymbol{b} \quad [17]$$

Equation 17 can be inverted to get

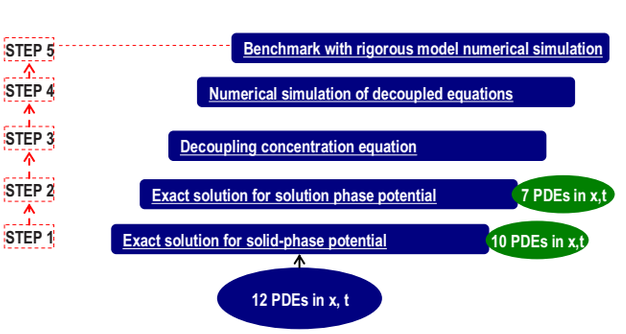

Figure 1. (Color online) Schematic of steps involved in reformulation using the finite-difference approach.

$$\mathbf{\Phi}_1 = \boldsymbol{A}^{-1}\boldsymbol{j}_p + \boldsymbol{A}^{-1}\boldsymbol{b} \quad [18]$$

When two node points in the x axis are used for discretization ($N = 2$), the discretized form of the equation is as follows. At $x = 0$, $i = 0$

$$\Phi 1_0 = 4.2 \quad [19]$$

For $0 < x < l_p$, $0 < i < 3$

$$\sigma_{\text{eff,p}}\frac{\Phi 1_2 - 2\Phi 1_1 + \Phi 1_0}{h_1^2} = a_p F j_{p1} \quad [20]$$

$$\sigma_{\text{eff,p}}\frac{\Phi 1_3 - 2\Phi 1_2 + \Phi 1_1}{h_1^2} = a_p F j_{p2} \quad [21]$$

At $x = lp$, $i = 3$

$$-\sigma_{\text{eff,p}}\left[\frac{\Phi 1_1 - 4\Phi 1_2 + 3\Phi 1_3}{2h_1}\right] = 0 \quad [22]$$

For simplicity, Φ_2 and Φ_1 are written as $\Phi 2$ and $\Phi 1$, respectively, in the discretized equations. Typically, for linear boundary conditions, the value at the boundaries (0 and 3) for this case can be eliminated to obtain two coupled equations for two interior nodes as

$$\sigma_{\text{eff,p}}\frac{\Phi 1_2 - 2\Phi 1_1 + 4.2}{h_1^2} = a_p F j_{p1} \quad [23]$$

$$\sigma_{\text{eff,p}}\frac{2(\Phi 1_1 - \Phi 1_2)}{3h_1^2} = a_p F j_{p2} \quad [24]$$

The above set of equations can be written in matrix form as defined in Eq. 17 for the interior nodes 1 and 2. For two interior node points, the matrix inverse can be performed, and the solution is obtained as

$$\begin{bmatrix}\Phi 1_1\\ \Phi 1_2\end{bmatrix} = \frac{a_p F h_1^2}{\sigma_{\text{eff,p}}}\begin{bmatrix}-1 & -3/2\\ -1 & -3\end{bmatrix}\begin{bmatrix}j_{p1}\\ j_{p2}\end{bmatrix} - \begin{bmatrix}-1 & -3/2\\ -1 & -3\end{bmatrix}\begin{bmatrix}4.2\\ 0\end{bmatrix} \quad [25]$$

When three interior node points are used, the analytical solution is

$$\begin{bmatrix}\Phi 1_1\\ \Phi 1_2\\ \Phi 1_3\end{bmatrix} = \frac{a_p F h_1^2}{\sigma_{\text{eff,p}}}\begin{bmatrix}-1 & -1 & -3/2\\ -1 & -2 & -3\\ -1 & -2 & -9/2\end{bmatrix}\begin{bmatrix}j_{p1}\\ j_{p2}\\ j_{p3}\end{bmatrix} - \begin{bmatrix}-1 & -1 & -3/2\\ -1 & -2 & -3\\ -1 & -2 & -9/2\end{bmatrix} \times \begin{bmatrix}4.2\\ 0\\ 0\end{bmatrix} \quad [26]$$

Typically, 50 node points might be needed (and used) in the literature for getting a converged solution. Matrix methods can be used to derive and store the inverse matrix and solution a priori in the computer to eliminate the need for keeping Φ_1 in the model equations.[24,25] This way, we can reduce the number of variables in each electrode to be four. A general expression can be obtained for eigenvalues and eigenvectors as a function of N, the number of node points, so that there is no loss of accuracy while performing this step. For the original equation with the boundary conditions, the analytical solution for the eigenvalue is

$$\lambda_i = 2\left\{1 - \cos\left[\frac{\pi(2i-1)}{(2N+1)}\right]\right\}, \quad i = 1 \ldots N \quad [27]$$

Even though similar equations can be derived for eigenvectors as a function of N, the number of interior node points, a numerical approach might be more efficient (Ref. 24 and references therein). This step does not introduce any error (by developing a code that is generic for any number of node points, this step is equivalent to having an infinite number of node points and near-zero error for spatial discretization). Importantly, this step reduces the number of equations from 12 to 10 PDEs.

Analytical solution for solution-phase potential.— The first-order equation in Table I is the governing equation for the electrolyte potential. The nonlinear conductivity complicates the equation further. The linear term for the electrolyte potential gradient is taken to the left side, and finite difference is applied as explained for the solid-phase potential

$$-\frac{d\Phi_2}{dx} = \frac{i_{\text{app}}}{\kappa_{\text{eff,p}}} + \frac{\sigma_{\text{eff,p}}\dfrac{d\Phi_1}{dx}}{\kappa_{\text{eff,p}}} - \frac{2RT(1-t_+)}{F}\frac{d\ln c}{dx} \quad [28]$$

Unlike Φ_1, Φ_2 is relevant to all three regions, and both the variable Φ_2 and the electrolyte current density are continuous at the cathode/separator and separator/anode interface. However, during galvanostatic conditions, the current density at the interface is equal to the applied current density (solid-phase current is zero at the cathode/separator and separator/anode interface). This helps in solving for each of the regions independently. This step does not introduce any error as discussed earlier for the solid-phase potential. If finite difference is applied in the x direction, Eq. 28 can be written as

$$-\frac{1}{2}\frac{\Phi 2_{i+1} - \Phi 2_{i-1}}{h} = \frac{i_{\text{app}}}{\kappa_{\text{eff,p}}} + \frac{1}{2}\frac{\sigma_{\text{eff,p}}(\Phi 1_{i+1} - \Phi 1_{i-1})}{h\kappa_{\text{eff,p}}} - \frac{RT(1-t_+)}{F}\frac{(c_{i+1} - c_{i-1})}{hc_i} \quad [29]$$

where N is the number of interior node points used. Equation 29 can be written in matrix form as

$$\boldsymbol{A}_2\mathbf{\Phi}_2 = \mathbf{B}_1\mathbf{\Phi}_1 + \boldsymbol{b}_1\boldsymbol{f} + \boldsymbol{b}_2 \quad [30]$$

Using Eq. 8, we have

$$\mathbf{\Phi}_2 = \boldsymbol{A}_{2\_}^{-1}\boldsymbol{B}_2\boldsymbol{j}_p + \boldsymbol{A}_{2\_}^{1}\boldsymbol{B}_3\boldsymbol{f} \quad [31]$$

where $\boldsymbol{B}_2$ is obtained from Eq. 8, $\boldsymbol{f}$ is a nonlinear function of other dependent variables resulting from the governing equation, and $\boldsymbol{B}_3$ is another nonlinear function in c that combines $\boldsymbol{b}_1$ and $\boldsymbol{b}_2$ at various node points in x. If electrolyte conductivity is assumed as a constant, then Eq. 31 would be easier to solve.

When two node points in the x axis are used for discretization ($N = 2$), the discretized form of the equation is as follows. At $x = 0$, $i = 0$

$$\frac{1}{2}\frac{-\Phi 2_2 - 3\Phi 2_0 + 4\Phi 2_1}{h} = 0 \quad [32]$$

For $0 < x < l_p$, $0 < i < 3$

$$-\frac{1}{2}\frac{\Phi 2_2 - \Phi 2_0}{h} = \frac{i_{\text{app}}}{\kappa_{\text{eff,p}}} + \frac{1}{2}\frac{\sigma_{\text{eff,p}}(\Phi 1_2 - \Phi 1_0)}{h\kappa_{\text{eff,p}}} - \frac{RT(1-t_+)}{F}\frac{(c_2 - c_0)}{hc_1} \quad [33]$$

$$-\frac{1}{2}\frac{\Phi 2_3 - \Phi 2_1}{h} = \frac{i_{\text{app}}}{\kappa_{\text{eff,p}}} + \frac{1}{2}\frac{\sigma_{\text{eff,p}}(\Phi 1_3 - \Phi 1_1)}{h\kappa_{\text{eff,p}}} - \frac{RT(1-t_+)}{F}\frac{(c_3 - c_1)}{hc_2} \quad [34]$$

At $x = lp$, $i = 3$

$$-\frac{1}{2}\frac{\Phi 2_1 + 3\Phi 2_3 - 4\Phi 2_2}{h} = \frac{i_{\text{app}}}{\kappa_{\text{eff,p}}} \quad [35]$$

This yields the solution for electrolyte potential at various node points and at various regions by following the same. Note that depending on the selection of discretization approaches and boundary conditions, the resulting matrices might be singular (with just one eigenvalue = 0). These systems can be handled by arbitrarily setting $\Phi 2$ = constant at the interfaces and then solving numerically for an additional equation that relates flux to the current density at the

interface. Importantly, this step reduces the number of equations from 10 to 7 PDEs.

Decoupling concentration equations.— At this stage, only c has to be solved in all the regions with additional nonlinear algebraic equations defined from the previous steps. If finite differences are applied in the spatial direction for all the regions, the discretized form can be written in matrix form (after substituting the parameters of the system and eliminating the concentration values at the interfaces) as

$$\begin{bmatrix} \frac{d\bar{c}_1}{dt} \\ \frac{d\bar{c}_2}{dt} \\ \frac{d\bar{c}_3}{dt} \\ \frac{d\bar{c}_4}{dt} \\ \frac{d\bar{c}_5}{dt} \\ \frac{d\bar{c}_6}{dt} \end{bmatrix} = \begin{bmatrix} -0.0401 & 0.04012 & 0 & 0 & 0 & 0 \\ 0.0597 & -0.1184 & 0.0783 & -0.0196 & 0 & 0 \\ -0.0333 & 0.1332 & -2.8665 & 2.7657 & 0 & 0 \\ 0 & 0 & 2.8064 & -3.0281 & 0.2957 & -0.0739 \\ 0 & 0 & -0.0314 & 0.01254 & -0.1917 & 0.0976 \\ 0 & 0 & 0 & 0 & 0.0663 & -0.0663 \end{bmatrix} \begin{bmatrix} \bar{c}_1 \\ \bar{c}_2 \\ \bar{c}_3 \\ \bar{c}_4 \\ \bar{c}_5 \\ \bar{c}_6 \end{bmatrix} + \begin{bmatrix} 1464272.72 & 0 & 0 & 0 & 0 & 0 \\ 0 & 1464272.72 & 0 & 0 & 0 & 0 \\ 0 & 0 & 0 & 0 & 0 & 0 \\ 0 & 0 & 0 & 0 & 0 & 0 \\ 0 & 0 & 0 & 0 & 950377.73 & 0 \\ 0 & 0 & 0 & 0 & 0 & 950377.73 \end{bmatrix} \begin{bmatrix} j_{p1} \\ j_{p2} \\ 0 \\ 0 \\ j_{n1} \\ j_{n2} \end{bmatrix} \quad [36]$$

This can be denoted as

$$\frac{d\mathbf{c}}{dt} = B\mathbf{c} + b\mathbf{j} \quad [37]$$

The coefficient matrix handles the flux continuity at the interfaces and the boundary conditions. An analytical solution for this matrix is much more complicated than the previous case. Matrix simulation for various values of node points N (same node points used in each region) can be run, and an empirical relationship for eigenvalues can be found as a function of N. Standard numerical methods for finding eigenvalues of banded matrices can be performed in advance in a computer to be stored and used for various simulations.[24,26] These values can be tested by comparing with rigorous numerical calculations for the matrix for various values of N. This will help in decoupling the equations, which will make the simulation much more efficient instead of solving the equations directly. When two node points in the x axis are used for discretization ($N = 2$) in all three regions, the discretized form of the governing equation can be written in the matrix form shown in Eq. 36. The form of Eq. 36 and its eigenvalues/eigenvectors are independent of the value of the applied current density.

The eigenvalues for the **B** matrix can be found as follows

$$\lambda = [-5.739475381 \quad -0.3184711833 \quad -0.1606699925 \quad 0.00000000016 \quad -0.07270344595 \quad -0.01902588106] \quad [38]$$

(Note that one of the eigenvalues is indeed zero. However, because of numerical errors in matrix manipulations, a small value can help in avoiding the singularity). Equation 37 can now be written as

$$\frac{d\mathbf{c}}{dt} = P\lambda P^{-1}\mathbf{c} + b\mathbf{j} \quad [39]$$

If $\boldsymbol{P}^{-1}\boldsymbol{c} = \bar{c}$, this simplifies Eq. 29 as

$$\frac{d\bar{\mathbf{c}}_i}{dt} = \lambda_i\bar{\mathbf{c}}_i + B_4\mathbf{j}_i \quad [40]$$

The form of Eq. 30 for $i = 1$ is given as

$$\frac{d\bar{c}_1}{dt} = -5.739475381\bar{c}_1 + 4300.157028j_{p1} - 16758.95072j_{p2} + 25052.24504j_{n5} - 6536.712142j_{n6} \quad [41]$$

Similar equations can be derived for other eigen-nodes and $\bar{c}$. Note that for $N = 100$ or 200 node points, matrix equations can be performed in Maple, stored and used for future purposes, or called to a Fortran file. The corresponding author would be happy to provide sample Maple codes that address this concept.

Numerical simulation of decoupled equations.— At this stage, even if 50 node points are used in each region, the resulting 150 decoupled equations for c coupled with 100 decoupled algebraic equations for $c_{s,surf}$ or $j_{p/n}$ and 100 decoupled ordinary differential equations (ODEs) for $c_{s,ave,p/n}$ (which occurs only in the electrode) can be solved efficiently in Fortran. After this step, the reformulated models can be run in less than 100 ms as required in a hybrid environment, which might have supercapacitors with time constants less than 1 s. Two different approaches are proposed to perform numerical simulation of decoupled equations, (*i*) direct simulation of resulting DAEs using DASSL[27] or similar solvers and (*ii*) the decoupled equation for concentration, integrated as

$$c_i = c_{i_0} \exp(\lambda_i t) + \int_0^\tau \exp[\lambda_i (t-\tau)][B_4 j_p]_i dt \quad [42]$$

The integration is carried out by choosing certain numbers of discretized or Gaussian points in t. This yields a system of nonlinear algebraic equations which can be readily solved. Note that the calculation of integrals involving higher-order eigenvalues can be obtained by performing suitable approximations/transformations on the first few integrals.

Benchmarking.— The reformulated models are tested with the full-order model (with approximation for the solid phase) used in the literature. Both external/system (voltage–time curve, process variable) and internal variables are expected to match exactly for rates less than 2C. One can imagine the difficulty with the finite difference/volume/element approaches in solving the rigorous model. Matrix methods are needed to find the eigenvalues and eigenvectors as a function of N, the number of node points. Unfortunately, we could not find any patterns reported in the literature for banded matrices in mixed domains (cathode/separator/anode) with varying diffusion coefficients in each region. Finding eigenvalues as a closed-form expression as in Eq. 27 is called "pattern" in math literature.[24-26] While it is possible that a pattern exists, numerical analysis can be performed to obtain them empirically as a function of N. Our experience suggests that finite difference is not the best possible approach for the reformulation. The details are provided in this manuscript for the readers to avail this approach if they prefer to stick to finite-difference reformulation. In the next section, we show how polynomial representation can be used to implement model reformulation.

Reformulation based on polynomial representation.— Solid-phase potential.— Instead of finite differences, if j_p is assumed to be a sum of polynomials or functions given by

$$j_p = \sum_{i=0}^{N} \alpha_{pi} f_i(x) \quad [43]$$

where $f_i(x)$ is a function in x, Eq. 11 can be integrated in x to obtain

$$\Phi_1 = c_1 + c_2 x + \frac{a_p F}{\sigma_{eff,p}} \sum_{i=0}^{N} \alpha_{pi} \int \left[\int f_i(x) dx \right] dx \quad [44]$$

In the literature, various kinds of polynomials have been used for model reformulation (e.g., Chebyshev polynomials,[20] proper orthogonal decomposition,[23] etc.). If the functions chosen have exact double integrals, we have an analytical solution for this equation which is valid as long as enough terms are chosen in Eq. 43. If simple polynomials are chosen, j_p is given by

$$j_p = \sum_{i=0}^{N} \alpha_{pi} x^i \quad [45]$$

and Φ_1 is given by

$$\Phi_1 = c_1 + c_2 x + \frac{a_p F}{\sigma_{eff,p}} \sum_{i=0}^{N} \alpha_{pi} \frac{x^{i+2}}{(i+1)(i+2)} \quad [46]$$

The integration constants in Eq. 43 or 46 are solved using the boundary conditions

$$\Phi_1|_{x=0} = 4.2 \quad [47]$$

$$-\sigma_{eff,p} \left. \frac{\partial \Phi_1}{\partial x} \right|_{x=l_p} = 0 \quad [48]$$

For the above boundary conditions, the constants are (using Eq. 46)

$$c_1 = 4.2 \text{ and } c_2 = -\frac{a_p F}{\sigma_{eff,p}} \sum_{i=0}^{N} \frac{\alpha_{pi} l_p^{i+1}}{(i+1)} \quad [49]$$

From this analysis, it is clear that using polynomial for j_p is more advantageous than using the finite difference, finite element, or finite volume methods for reformulating Φ_1. It is advantageous because double integration to get Φ_1 is easier compared to inverting matrices in the finite-difference approach, which involves keeping track of eigenvalues, eigenvectors, or matrix inversions. Using one of the reformulation approaches outlined above, an analytical solution can be derived for the solid-phase potential distribution in each porous electrode. This reformulation process enables a closed-form solution for solid-phase potential distribution in each electrode as a function of other dependent variables without compromising on accuracy and without losing any physics of the battery system. Moreover, this reformulation technique reduces one PDE to one algebraic equation. At this stage, the original model for solid-phase potential is reduced to

$$\Phi_1(x) = 4.2 + \frac{a_p F}{\sigma_{eff,p}} \sum_{i=0}^{N} \frac{\alpha_{pi}}{i+1} \left\{ \frac{x^{i+2}}{i+2} - l_p^{i+1} \right\} \quad [50]$$

Solution-phase potential.— The governing equation for solution-phase potential is given by modified Ohm's law. If $\kappa_{eff,p}$ is a constant, clearly the governing equation for electrolyte potential can be solved analytically, yielding (assuming t_+ is a constant)

$$\Phi_2(x) = c_1 - \frac{I}{\kappa_{eff,p}} x - \frac{\sigma_{eff,p}}{\kappa_{eff,p}} \Phi_1(x) + \frac{2RT}{F}(1-t_+) \ln c \quad [51]$$

However, $\kappa_{eff,p}$ is a nonlinear function of the dependent variable (electrolyte concentration) for various chemistries. For example, for Li-ion chemistry where the electrolyte consists of 1 M LiPF6 in a mixture of ethylene carbonate:ethyl methyl carbonate, it is typically expressed as

$$\kappa_{eff,p} = \varepsilon_p^{brugg_p}(4.1253 \times 10^{-2} + 5.007 \times 10^{-4} c - 4.7212 \times 10^{-7} c^2 + 1.5094 \times 10^{-10} c^3 - 1.6018 \times 10^{-14} c^4) \quad [52]$$

where c is a function in x. Equation 52 can now be integrated in x to obtain (assuming t_+ to be a constant)

$$\Phi_2(x) = k_1 - I \int_x \frac{1}{\kappa_{eff,p}} dx - \sigma_{eff,p} \int_x \frac{1}{\kappa_{eff,p}} \frac{\partial \Phi_1}{\partial x} dx + \frac{2RT}{F}(1-t_+) \ln c \quad [53]$$

provided I, the applied current, is a constant (true for galvanostatic boundary conditions). If the function governing the variation of $1/\kappa_{eff,p}$ with respect to other dependent variables has an exact integral, we have an analytical solution for this equation. If not, simple polynomials are chosen for $1/\kappa_{eff,p}$ given by

$$\frac{1}{\kappa_{eff,p}} = \sum_{i=0}^{N} \zeta_{pi} x^i \quad [54]$$

and Φ_2 can be solved as

$$\Phi_2(x)|_{cathode} = k_1 - I \sum_{i=0}^{N} \zeta_{pi} \frac{x^{i+1}}{i+1} - \sigma_{eff,p} \Gamma + \frac{2RT}{F}(1-t_+) \ln c \quad [55]$$

where Γ is a product of two summation series resulting from integration. The respective boundary and initial conditions are used, including the continuous-flux boundary conditions at the electrode/separator or separator/electrode interfaces to solve for constants. In addition, the Galerkin-type-collocation weighted average method is used to solve for the constants.[15,16] For example, each constant ζ_{pi} is obtained by minimizing the residue of the governing equation with a

weighting function given by the coefficient of the particular constant as

$$\frac{1}{l_p}\int_{x=0}^{l_p} w_1 Ge(\Phi_2)|_{\text{cathode}}dx + \frac{1}{l_s}\int_{l_p}^{l_p+l_s} w_2 Ge(\Phi_2)|_{\text{separator}}dx + \frac{1}{l_n}\int_{l_p+l_s}^{L} w_3 Ge(\Phi_2)|_{\text{anode}}dx = 0 \quad [56]$$

where $w1$, $w2$, and $w3$ are the weight functions and $\text{Ge}(\Phi_2)$ denotes the governing equation of Φ_2. Note that six of the constants in the polynomials are obtained from the boundary conditions at $x = 0$, lp, $lp + ls$, and L. At the electrode/separator interfaces, both the electrolyte potential and its fluxes are continuous.

Solid-phase average concentration.— The solid-phase average concentration c_s^{ave} dependency with j_p (see Table I) can be decoupled by assuming polynomial representations as follows

$$c_{sp}^{\text{ave}} = \sum_{i=0}^{N} \beta_{pi}(t)x^i \quad [57]$$

Substituting Eq. 57 in the governing equation for solid-phase average concentration and equating like terms on both sides gives

$$\frac{d}{dt}\beta_{pi}(t) = -\frac{3}{R_p}\alpha_{pi} \quad i = 0 \ldots N \quad [58]$$

The system of ODEs given by Eq. 58 can be solved to obtain solid-phase average concentration distribution across the porous electrode. This system of ODEs is computationally more efficient to solve than solving the original governing equation for solid-phase average concentration directly because of the decoupled nature.

Pore-wall flux.— The series assumed for pore-wall flux is

$$j_p = \sum_{i=0}^{N} \alpha_{pi}x^i \quad [59]$$

The constants are obtained using Galerkin-type collocation

$$\int_0^{l_p} w(x)Ge(j_p)dx = 0 \quad [60]$$

To speed up the convergence of the polynomial representation, the average value for j_p is used as an additional constraint. The average value for j_p is obtained using the governing equation for solid-phase potential. Integrating over the positive electrode, we have

$$\sigma_{\text{eff,p}}\frac{\partial\Phi_1}{\partial x}\bigg|_{x=l_p} - \sigma_{\text{eff,p}}\frac{\partial\Phi_1}{\partial x}\bigg|_{x=0} = -a_pFj_p^{\text{ave}}l_p \quad [61]$$

Using the boundary condition for Φ_1, this can be written as[14,21]

$$j_p^{\text{ave}} = -\frac{i_{\text{app}}}{a_pFl_p} \quad [62]$$

This average pore-wall flux provides and paves the way for quicker convergence for the polynomial representation. Similarly, the average flux at the negative electrode can be derived as

$$j_n^{\text{ave}} = \frac{i_{\text{app}}}{a_nFl_n} \quad [63]$$

Electrolyte concentration.— The governing equations for electrolyte concentration are derived from Fick's law of mass transport and concentrated solution theory and are given as Eq. 1, 15, and 17 in Table I for the positive electrode, separator, and negative electrode, respectively. The dependent variable for each region is approximated with polynomial expressions as

$$c = \sum_{i=0}^{N} \psi_i(t)x^{i+1} \quad [64]$$

Equation 52 can be substituted into the governing equation for electrolyte concentration to get

$$Gep = c(x)|_{\text{cathode}} = \varepsilon_p\sum_{i=0}^{N} x^{i+1}\frac{d}{dt}\psi_{pi}(t) - D_{\text{eff,p}}\left[\sum_{i=0}^{N}(i-1)ix^{i-2}\psi_{pi}(t)\right] - a_p(1-t_+)\sum_{i=0}^{N} a_ix^i \quad [65a]$$

$$Ges = c(x)|_{\text{separator}} = \varepsilon_s\sum_{i=0}^{N} x^{i+1}\frac{d}{dt}\psi_{si}(t) - D_{\text{eff,s}}\left[\sum_{i=0}^{N}(i-1)ix^{i-2}\psi_{si}(t)\right] \quad [65b]$$

$$Gen = c(x)|_{\text{anode}} = \varepsilon_n\sum_{i=0}^{N} x^{i+1}\frac{d}{dt}\psi_{ni}(t) - D_{\text{eff,n}}\left[\sum_{i=0}^{N}(i-1)ix^{i-2}\psi_{ni}(t)\right] - a_n(1-t_+)\sum_{i=0}^{N} a_ix^i \quad [65c]$$

Equation 65 is then used to arrive at individual equations using Galerkin collocation as

$$\frac{1}{l_p}\int_{x=0}^{l_p} w_1 Gepdx + \frac{1}{l_s}\int_{l_p}^{l_p+l_s} w_2 Gesdx + \frac{1}{l_n}\int_{l_p+l_s}^{L} w_3 Gendx = 0 \quad [66]$$

As before for electrolyte potential, six of the constants in the polynomials are found using the boundary conditions. In addition, volume averaging can be performed to the original set of PDEs.

The electrolyte concentration can be volume-averaged over the respective region as follows

$$\varepsilon_p\int_{x=0}^{l_p}\frac{\partial c}{\partial t}dx + \varepsilon_s\int_{x=l_p}^{l_p+l_s}\frac{\partial c}{\partial t}dx + \varepsilon_n\int_{x=l_p+l_s}^{L}\frac{\partial c}{\partial t}dx = D_{\text{eff,p}}\left(\frac{\partial c}{\partial x_{x=l_p}} - \frac{\partial c}{\partial x_{x=0}}\right) + a_p(1-t_+)\int_{x=0}^{l_p} j_p dx + D_{\text{eff,s}}\left(\frac{\partial c}{\partial x_{x=l_p+l_s}} - \frac{\partial c}{\partial x_{x=l_p}}\right) + D_{\text{eff,n}}\left(\frac{\partial c}{\partial x_{x=L}} - \frac{\partial c}{\partial x_{x=l_p+l_s}}\right) + a_n(1-t_+)\int_{x=l_p+l_s}^{L} j_n dx \quad [67]$$

This can be simplified using the boundary conditions to get

$$\varepsilon_p l_p\frac{dC_{\text{ave}}^{\text{Cathode}}}{dt} + \varepsilon_s l_s\frac{dC_{\text{ave}}^{\text{Separator}}}{dt} + \varepsilon_n l_n\frac{dC_{\text{ave}}^{\text{Anode}}}{dt} = 0 \quad [68]$$

This can be integrated to obtain

$$C_{\text{ave}}^{\text{Total}} = \frac{\varepsilon_p C_{\text{ave}}^{\text{Cathode}} + \varepsilon_s C_{\text{ave}}^{\text{Separator}} + \varepsilon_n C_{\text{ave}}^{\text{Anode}}}{\varepsilon_p l_p + \varepsilon_s l_s + \varepsilon_n l_n} = 1000 \quad [69]$$

This is true for any chemistry and can also be derived from overall mass balance of the cell. This provides for and facilitates a quicker convergence of concentration profiles in terms of polynomials. If this condition is not used, a higher number of terms may be needed in the polynomial representation, and the polynomial representation might even be unstable for a lower number of terms.

The initial conditions for solving the system of ODEs represented by Eq. 66 are given as

$$\psi_i(0) = c_0 \quad i = 0 \ldots N \quad [70]$$

For improved efficiency, the decoupled system of equations is arrived from Eq. 56 by writing the system of equations in matrix form and decoupling the same

$$\frac{d\psi_i}{dt} = f(\varepsilon, D, t_+, a, \psi_{i=0\ldots N}, \alpha_{i=0\ldots N}) \text{ for each } i = 0 \ldots N \quad [71]$$

At this stage, if $N = 4$ is chosen for Eq. 58 and 71, then the model for each electrode is reduced to $4 + 4 + 1 + 1 + 1 = 11$ DAEs. This yields $11 + 5 + 11 = 27$ DAEs for the full model. If $N = 8$ is chosen for Eq. 58 and 71, then the model for each electrode becomes $8 + 8 + 1 + 1 + 1 = 19$ DAEs. This yields $19 + 9 + 19 = 47$ DAEs for the rigorous full model.

This means that for lithium-ion battery modeling, we now need to solve only $4 \times 3 + 4 \times 2 + 3 \times 1 + 2 \times 1 + 2 \times 1 = 27$ DAEs or 27-47 DAEs, depending on matching the discharge curve alone or matching the entire profile output with the rigorous numerical simulation for up to 2C rate of charge/discharge. These equations are solved using DASSL, a DAE solver, to obtain discharge curves.[27]

By using the approximations discussed in this paper, we are able to predict the discharge curves accurately with just 47 DAEs. Note that 47 DAEs are needed for matching for all the intrinsic variables. With our approach we can choose to go "approximate" in the intrinsic variables and solve only discharge curves accurately with only 27 DAEs.

These models take 30 s to 2 min to run in a Maple environment using a DAE solver called Besirk.[28] A variant of the same model runs in 15–50 ms in a Fortran environment to predict an entire discharge curve (1.7 GHz processor and 1 GB RAM). To predict state of charge at a particular time, the time taken is of the order of 5–10 ms. The reformulated models have been tested for rates up to 2C, and work is in progress for the process of testing for rates up to 50C (for higher rates, solid-phase approximation needs to be redefined). The efficiency of the reformulation can be further improved using the Liaponuv–Schmidt technique, dimensional analysis, perturbation, etc., as discussed in the earlier work.[21]

Results and Discussion

Model reformulation.— Discharge behavior of lithium-ion batteries is the prime goal of the simulation performed in this paper. Figure 2 gives the discharge curves for 1C (30 A/m^2) and 0.5C rates of galvanostatic discharge. For these rates of discharge, the reformulated model compares well with the full-order numeric model. The merit of this approach is evident when comparing the number of governing equations that are solved. The reformulated model specifies 47 DAEs as opposed to 250 DAEs for the rigorous model. Also, 250 DAEs is the minimum number of equations required for a converged finite difference solution of the full-order model. The reformulated model for all practical situations (rates of discharge) uses a maximum of 47 specified equations for a converged solution, which compares well even with 250 DAEs based on the finite difference code.

The reformulated model also predicts the intrinsic variables accurately as shown in Fig. 3. The intrinsic variables, namely, overpotential (η), solution-phase potential (Φ_2), pore-wall flux (j_p/j_n), and

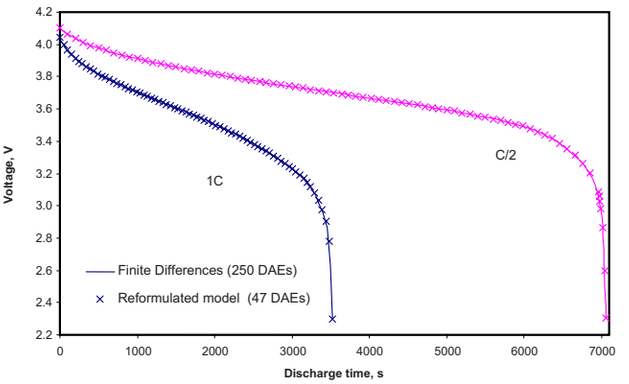

Figure 2. (Color online) Discharge curve for 1C and 0.5C rate comparing the rigorous numerical model and reformulated model based on polynomial representation. There is good agreement between the two models.

electrolyte concentration (c), determined by the reformulated model are plotted and compared with the results generated from a rigorous finite-difference code. The interfaces are the positive electrode–current collector junction ($x = 0$), the positive electrode–separator

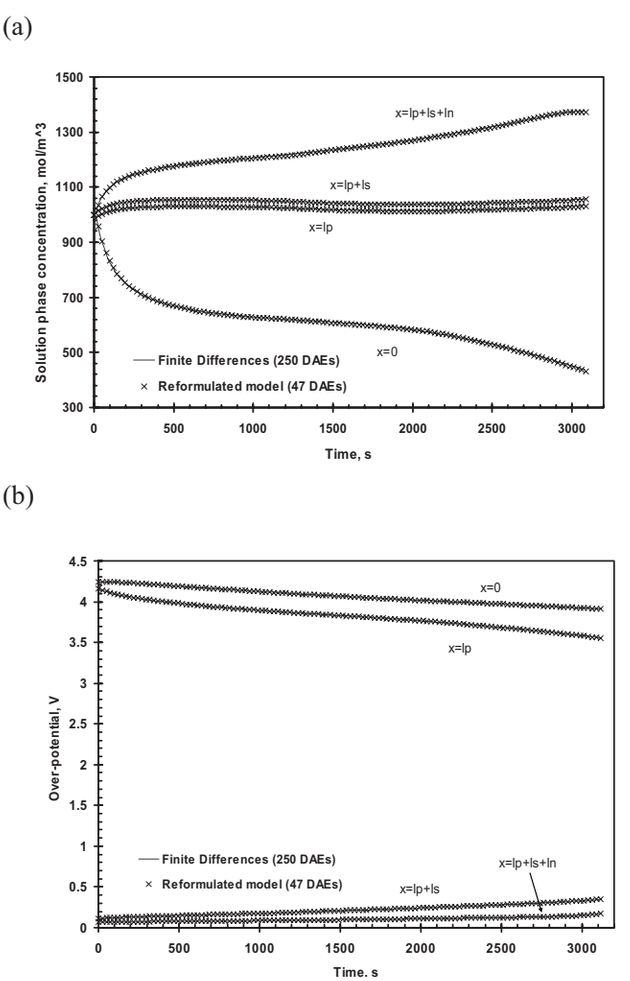

Figure 3. Solution-phase concentration and overpotential η at different times for 1C rate at different interfaces comparing the rigorous numerical model and reformulated model based on polynomial representation. There is good agreement between the two models.

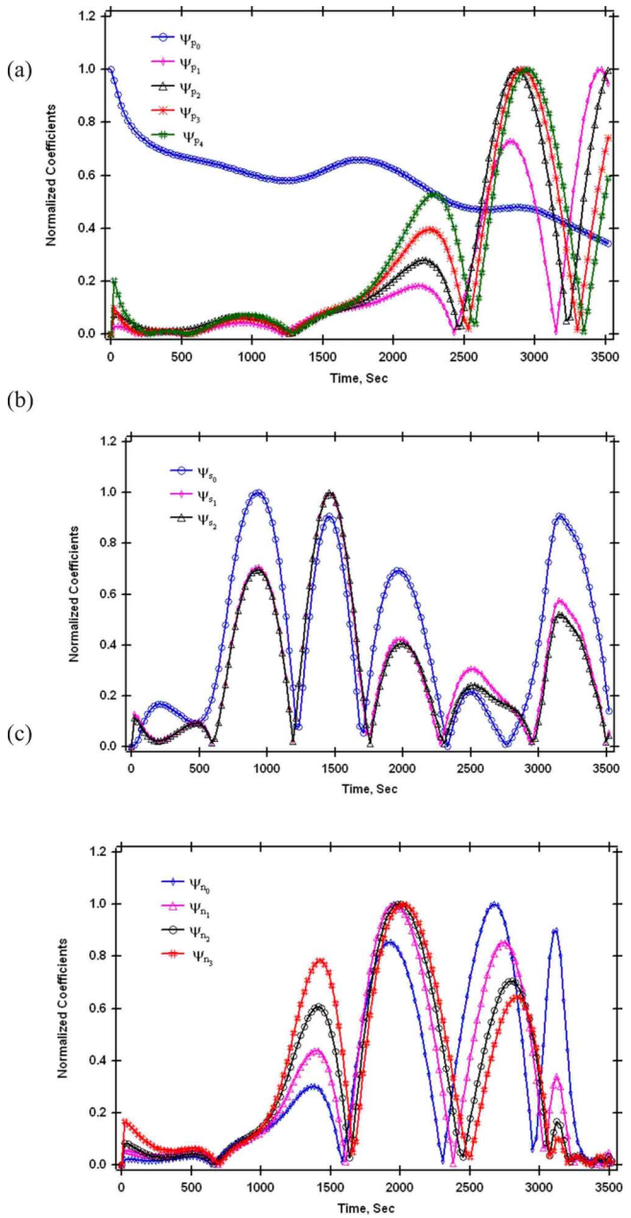

Figure 4. (Color online) (a) Positive electrode, (b) separator, and (c) negative electrode. Dynamic behavior of the coefficients in series solution for electrolyte concentration at 1C rate of discharge used for the reformulated model based on polynomial representation.

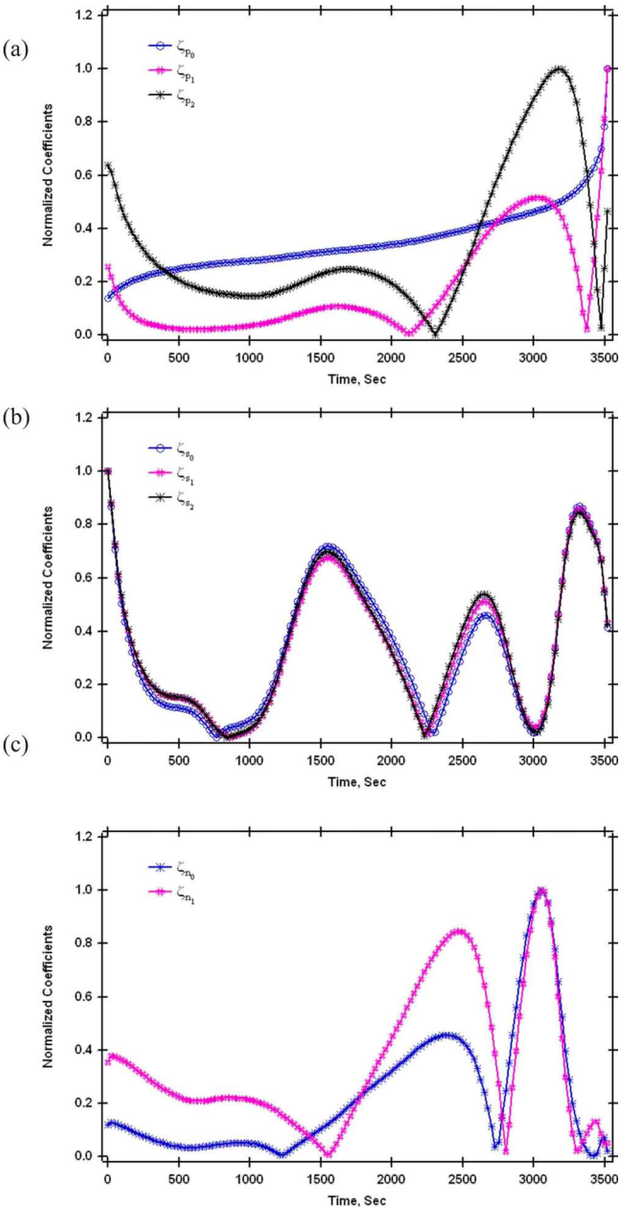

Figure 5. (Color online) (a) Positive electrode, (b) separator, and (c) negative electrode. Dynamic behavior of the coefficients in series solution for electrolyte potential at 1C rate of discharge used for the reformulated model based on polynomial representation.

(electrolyte) junction ($x = l_p$), the separator–negative electrode junction ($x = l_p + l_s$), and the negative electrode–current collector junction ($x = l_p + l_s + l_n$). It has been clearly seen that the reformulated model saves computational time without compromising the physics of the system.

The coefficients of polynomial used to approximate the electrolyte concentration c, the electrolyte potential Φ_2, the solid-phase surface concentration $j_{p/n}$, and the solid-phase surface concentration $c_{s,avg,p/n}$ are plotted in Fig. 4-7 as a function of time. The coefficients in the polynomial for various dependent variables are normalized (to its maximum value). From these figures it is clear that significant changes happen over time for all the coefficients, but a good pattern in time is observed, suggesting future reformulation based on assumed profiles in time for the dependent variables.

Convergence and stability.— The method proposed here is analytical for the algebraic variables and polynomial approximation for the differential variables. In addition to Galerkin collocation, volume averaging the original equation provides the average concentration in each region related to the overall average concentration and the initial condition and the average pore-wall fluxes in the positive and negative electrodes. This condition helps in getting the polynomial representation to converge faster. The method reported is found to be stable based on testing the same for various chemistries and rates. However, the reformulated code is highly sensitive to the initial conditions for the algebraic variables, and an analytical Jacobian might be needed for the DAE solver.

Parameter estimation.— The reformulated model retains the physics of the original model. Because of this, parameter estimation can be done confidently.[29] Figure 8 compares the prediction of trans-

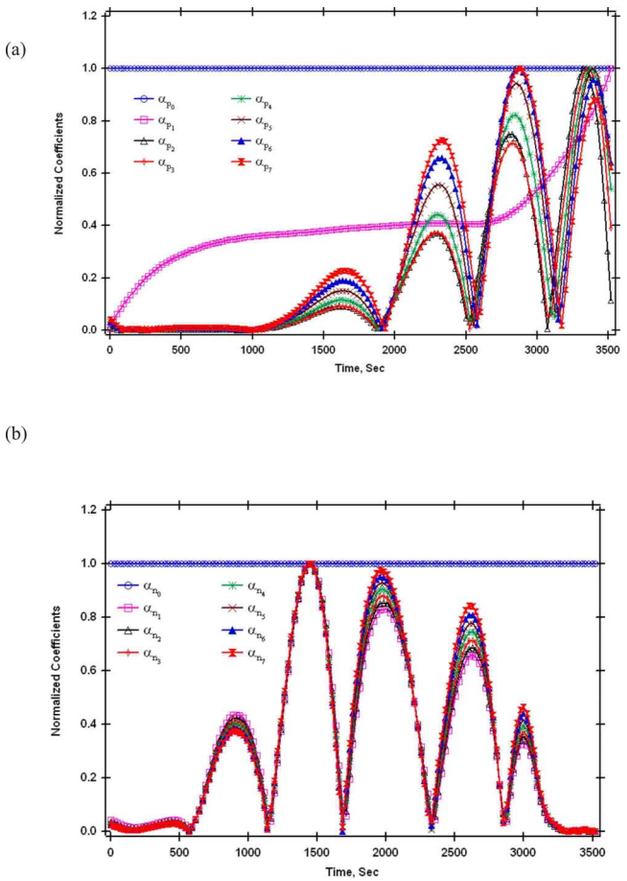

Figure 6. (Color online) (a) Positive electrode and (b) negative electrode. Dynamic behavior of the coefficients in series solution for electrochemical reaction kinetics at 1C rate of discharge used for the reformulated model based on polynomial representation.

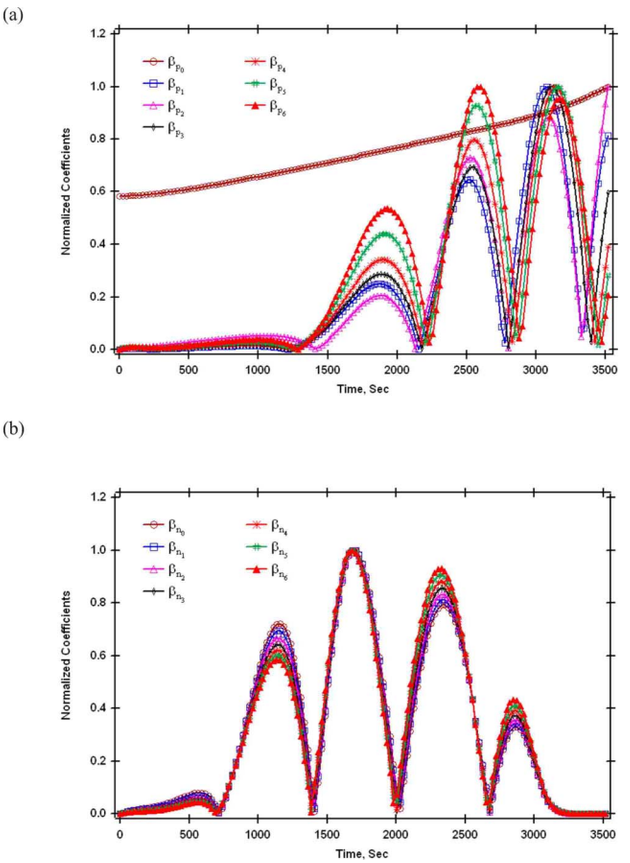

Figure 7. (Color online) (a) Positive electrode and (b) negative electrode. Dynamic behavior of the coefficients in series solution for solid-phase average concentration at 1C rate of discharge used for the reformulated model based on polynomial representation.

port and kinetic parameters with the reformulated model from the experimental data for the cells from Quallion LLC. It is clear that for life data prediction, the reformulated model can be more advantageous.

Because of the accuracy and simplicity of the reformulated model, sensitivity equations can be derived easily, and even the numerical Jacobian is likely to be more accurate and stable compared to the original finite-difference form of the model.

Generality and limitations.— Clearly, the method presented here is directly applicable for charging also, as it only changes the sign of the applied current density. As mentioned earlier, the readers are advised that the volume-averaged equations are not valid at short times and pulse charges/discharges. The solid-phase equations should be reformulated in efficient form before reformulation is done for the other variables. However, this paper focuses on reformulation in the x direction, and hence the discussion is limited to volume-averaged equations for the solid-phase equation. A good comparison of various approximations for solid-phase reformulation is presented elsewhere in the literature[15,16] and that approach provides high efficiency at short times. A mixed-order finite element was proposed and is probably the best possible approach at this point in time. However, their approach uses a discretization scheme in time which restricts the approach for standard discretization schemes and is not applicable for DASSL-type adaptive solvers, which cannot handle time-discretized equations. A similar form can be constructed from mixed-order finite difference which is found to be efficient even for varying diffusivities in time.[30]

Previous approaches[31] are robust and can handle high rates by adding more terms to the spectral solution equations. However, this solution increases to high numbers for the coefficients requiring stricter tolerances and lesser computational efficiency. An alternative, equivalent, and efficient form can be derived using a Galerkin-type integral.[30] The scope of this paper is restricted to volume-averaged equations for the solid phase.

For lumped parameter models for the temperature, an additional ODE can be solved in addition to the governing equations consid-

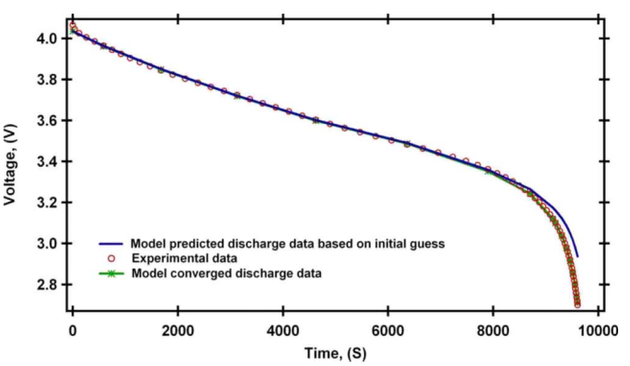

Figure 8. (Color online) Comparison of five-parameter prediction with the reformulated model based on polynomial representation to experimental data.

ered earlier. This does not affect the solution of solid and electrolyte phase potentials, pore-wall flux, the algebraic nature and its solution are still preserved. Arhenius-type behavior can be incorporated into the reformulated model equations even in a final stage with T as a time-varying variable as opposed to a parameter. If the objective is to find only temperature change, the intrinsic variables might be solved in an approximate manner. This is beyond the scope of this paper. If temperature variation with distance is not negligible across the distance, the parameters change with distance, and algebraic equations cannot be directly integrated. However, series expansions like the one used for $\kappa_{\text{eff,p}}$ can be employed.

If the operating mode is applied potential or applied power, the boundary conditions change. In this case, the constants of integrations are affected. The effect of resistance from the solid electrolyte interphase layer can be easily included by modifying the kinetic expression in the negative electrode. This should not affect the reformulated model. However, if moving boundaries are to be included, then the reformulated model has to account for the same.

Mathematical model reformulation for different boundary conditions (applied potential or power), temperature distribution, and moving boundaries will be communicated in future publications.

Perspectives and Future Work

In this paper, mathematical analysis is used to reduce the order and number of equations without compromising on accuracy and physics. The original model chosen is a reduced 1D model with volume-averaged approximation for the solid-phase equations. The methods described here are valid for battery models in the x direction, i.e., along the direction of movement of current from the cathode current collector to the anode current collector. Polynomial forms for j_{p} and j_{n}, the pore-wall flux, appear to be the best possible way to reformulate the original model. Clearly, different forms of the series representation can give better results and are currently being attempted by our group.

The model chosen (averaged equations for the solid-phase concentration) is valid only at low-to-medium rates of discharge. This proves to be advantageous while using DASSL-type solvers in time. For high rates of discharge, one might need a large number of node points or polynomials in r. At this number, the DASSL-type solver may not provide any advantage, and perhaps the linear equations can be solved analytically if simpler discretization schemes are used in time.

In addition, the plots for the coefficients in the polynomial for various dependent variables are normalized (to its maximum value) and plotted. From Fig. 4-7, it is clear that the averaged solid-phase concentration behaves the smoothest of all. This is expected, because the governing equation for the average solid-phase concentration (Eq. 4 in Table I) is an integral of the pore-wall flux. These figures also suggest that perhaps a double summation in x and t can be assumed for all the variables. The prudent way to approach this would be to attempt this for only one variable first and check for efficiency and convergence, then move forward for all the model equations. We are attempting to do this, and if we are successful we will report the results. For electrolyte concentration, different constants are used in the polynomial representations in each region (positive electrode, separator, and negative electrode). It is possible to arrive at eigenfunctions based on linearized versions of the models. The use of these eigenfunctions might reduce the number of constants needed in the polynomial representation.[32,33]

Conclusions

This paper presents an efficient approach to simulate discharge behavior of lithium-ion battery models for galvanostatic boundary conditions with improved computational efficiency using polynomial representation. The approach presented is similar to Galerkin collocation based on weighted residuals coupled with analytical solution of algebraic equations and volume-averaging for the variables of interest. The DAE nature of the model helps in solving for some of the dependent variables analytically. The model-reformulation method is demonstrated using low-to-moderate rates of discharge; however, the reformulation technique presented is also valid for different circumstances, including high rates of discharge and mass-transport-limited situations. This approach is currently in progress to enable the same level of computational efficiency while using multiple units or multiple power sources as needed in a hybrid system. The method reported here is likely to be valid and applicable for engineering models with DAE nature, including fuel cells, monolith reactors, etc. Source codes used for model reformulation in Maple or Matlab/Fortran will be posted on the corresponding author's website. Also, for control with microchips, RAM is likely to be a bigger concern compared to CPU time. A smaller number of DAEs and states should help in developing better controller algorithms.

Acknowledgments

The authors are thankful for the partial financial support of this work by the National Science Foundation (CBET–0828002), the U.S. Army Communications-Electronics Research, Development, and Engineering Center (CERDEC) under contract no. W909MY-06-C-0040, Oronzio de Nora Industrial Electrochemistry Postdoctoral Fellowship of The Electrochemical Society, and the United States government.

Author VRS thanks Professor John Newman, Department of Chemical Engineering, University of California, Berkeley for suggesting the need for computationally efficient battery models for process control purposes, Professor Ross Taylor at Clarkson University for developing and providing an efficient, robust, and user-friendly free DAE solver Besirk in Maple environment, and Professor Vemuri Balakotaiah at the University of Houston who had performed order reduction for monolith reactor models and from whom he had benefitted through e-mail communications.

Tennessee Technological University assisted in meeting the publication costs of this article.

List of Symbols

a_i	specific surface area of electrode i (i = p,n), m^2/m^3
$brugg_i$	Bruggman coefficient of region i (i = p,s,n)
c	electrolyte concentration, mol/m^3
c_0	initial electrolyte concentration, mol/m^3
$c_{s,i}$	concentration of lithium ions in the intercalation particle of electrode i (i = p,n), mol/m^3
$c_{s,i,0}$	initial concentration of lithium ions in the intercalation particle of electrode i (i = p,n), mol/m^3
$c_{s,i,\max}$	maximum concentration of lithium ions in the intercalation particle of electrode i (i = p,n), mol/m^3
D	electrolyte diffusion coefficient, m^2/s
$D_{s,i}$	lithium-ion diffusion coefficient in the intercalation particle of electrode i (i = p,n), m^2/s
F	Faraday's constant, C/mol
I	applied current density, A/cm^2
i_1	solid-phase current density, A/m^2
i_2	solution-phase current density, A/m^2
$i_{s,0}$	exchange current density for the solvent-reduction reaction, A/m^2
j_s	solvent-reduction current density, mol/m^2 s
j_i	wall flux of Li^+ on the intercalation particle of electrode i (i = n,p), mol/m^2 s
k_i	intercalation/deintercalation reaction-rate constant of electrode i (i = p,n), $mol/(mol/m^3)^{1.5}$
l_i	thickness of region i (i = p,s,n), m
M_s	molar weight of the solvent reaction product, g/mol
n	negative electrode
p	positive electrode
r	radial coordinate, m
R	universal gas constant, J/(mol K)
R_{SEI}	Initial SEI layer resistance at the negative electrode, $\Omega\ m^2$
R_i	radius of the intercalation particle of electrode i (i = p,n), m
s	separator
t_+	Li^+ transference number in the electrolyte
T	absolute temperature, K
U_i	open-circuit potential of electrode i (i = p,n), V
U_s	standard potential of the solvent reduction reaction, V
x	spatial coordinate, m

Greek

α,β,ζ,ψ	coefficients of polynomials used in model reformulation
δ	thickness of the solvent reduction product film, m
δ_0	initial thickness of the solvent reduction product film, m
ε_i	porosity of region i (i = p,s,n)
$\varepsilon_{f,i}$	volume fraction of fillers of electrode i (i = p,n)
θ_i	dimensionless concentration of lithium ions in the intercalation particle of electrode i ($\theta_i = c_{s,i}/c_{s,i,\max}$)
κ	ionic conductivity of the electrolyte, S/m
$\kappa_{\text{eff},i}$	effective ionic conductivity of the electrolyte in region i (i = p,s,n), S/m
ρ_s	density of the solvent reduction product film, g/m^3
σ_i	electronic conductivity of the solid phase of electrode i (i = p,n), S/m
$\sigma_{\text{eff},i}$	effective electronic conductivity of the solid phase of electrode i (i = p,n), S/m
Φ_1	solid-phase potential, V
Φ_2	electrolyte-phase potential, V

References

1. M. Doyle, T. F. Fuller, and J. Newman, *J. Electrochem. Soc.*, **140**, 1526 (1993).
2. J. Newman and W. Tiedemann, *AIChE J.*, **21**, 25 (1975).
3. T. F. Fuller, M. Doyle, and J. Newman, *J. Electrochem. Soc.*, **141**, 982 (1994).
4. T. F. Fuller, M. Doyle, and J. Newman, *J. Electrochem. Soc.*, **141**, 1 (1994).
5. M. Doyle, J. Newman, A. S. Gozdz, C. N. Schmutz, and J. M. Tarascon, *J. Electrochem. Soc.*, **143**, 1890 (1996).
6. K. E. Thomas and J. Newman, *J. Electrochem. Soc.*, **150**, A176 (2003).
7. P. Arora, M. Doyle, A. S. Gozdz, R. E. White, and J. Newman, *J. Power Sources*, **88**, 219 (2000).
8. P. Ramadass, B. Haran, R. E. White, and B. N. Popov, *J. Power Sources*, **123**, 230 (2003).
9. P. Ramadass, B. Haran, P. M. Gomadam, R. E. White, and B. N. Popov, *J. Electrochem. Soc.*, **151**, A196 (2004).
10. G. Ning, R. E. White, and B. N. Popov, *Electrochim. Acta*, **51**, 2012 (2006).
11. G. G. Botte, V. R. Subramanian, and R. E. White, *Electrochim. Acta*, **45**, 2595 (2000).
12. P. M. Gomadam, J. W. Weidner, R. A. Dougal, and R. E. White, *J. Power Sources*, **110**, 267 (2002).
13. S. Santhanagopalan, Q. Guo, P. Ramadass, and R. E. White, *J. Power Sources*, **156**, 620 (2006).
14. V. R. Subramanian, V. D. Diwakar, and D. Tapriyal, *J. Electrochem. Soc.*, **152**, A2002 (2005).
15. C. Y. Wang, W. B. Gu, and B. Y. Liaw, *J. Electrochem. Soc.*, **145**, 3407 (1998).
16. K. Smith and C. Y. Wang, *J. Power Sources*, **161**, 628 (2006).
17. V. Balakotaiah and S. Chakraborty, *Chem. Eng. Sci.*, **58**, 4769 (2003).
18. V. Balakotaiah and H.-C. Chang, *SIAM J. Appl. Math.*, **63**, 1231 (2003).
19. F. A. Howes and S. Whitaker, *Chem. Eng. Sci.*, **40**, 1387 (1985).
20. M. Golubitky and D. G. Schaeffer, *Singularities and Groups in Bifurcation Theory*, Vol. 1, Springer-Verlag, Berlin (1984).
21. V. R. Subramanian, V. Boovaragavan, and V. D. Diwakar, *Electrochem. Solid-State Lett.*, **10**, A225 (2007).
22. Institute of Mathematics, Technische University Berlin, http://www.math.tu-berlin.de//baur/D1.html, last accessed Jan 19, 2009.
23. L. Cai and R. E. White, Paper 107 presented at the Electrochemical Society Meeting, Phoenix, AZ, May 18–23, 2008.
24. V. R. Subramanian and R. E. White, *Chem. Eng. Sci.*, **59**, 781 (2004).
25. V. R. Subramanian and R. E. White, *Comput. Chem. Eng.*, **24**, 2405 (2000).
26. A. Varma and M. Morbidelli, *Mathematical Methods in Chemical Engineering*, Oxford University Press, New York (1999).
27. K. E. Brenan, S. L. Campbell, and L. R. Petzold, *Numerical Solution of Initial-Value Problems in Differential-Algebraic Equations*, North-Holland, New York (1989).
28. Department of Chemical Engineering, Clarkson University, http://people.clarkson.edu//chengweb/faculty/taylor/, last accessed Jan 19, 2009.
29. V. Boovaragavan, S. Harinipriya, and V. R. Subramanian, *J. Power Sources*, **183**, 361 (2008).
30. V. Ramadesigan, V. Boovaragavan, and V. R. Subramanian, *ECS Trans.*, **16**(29) (2009). In press.
31. Q. Zhang and R. E. White, *J. Power Sources*, **165**, 880 (2007).
32. V. R. Subramanian, J. A. Ritter, and R. E. White, *J. Electrochem. Soc.*, **148**, E444 (2001).
33. V. Boovaragavan, A. Guduru, V. Ramadesigan, and V. R. Subramanian, *J. Electrochem. Soc.*, To be submitted.